
EponaV2: Driving World Model with Comprehensive Future Reasoning

Jiawei Xu^{1,2}, Zhizhou Zhong^{2,3}, Zhijian Shu^{2,4}, Mingkai Jia^{2,3}, Mingxiao Li²,
 Jia-Wang Bian⁵, Qian Zhang², Kaicheng Zhang⁶, Jin Xie⁷, Jian Yang^{1,7}, Wei Yin²
¹PCA Lab, VCIP, College of Computer Science, Nankai University ²Horizon Robotics ³HKUST
⁴NJUPT ⁵NTU ⁶Anyverse ⁷School of Intelligence Science and Technology, Nanjing University

Abstract

Data scaling plays a pivotal role in the pursuit of general intelligence. However, the prevailing perception-planning paradigm in autonomous driving relies heavily on expensive manual annotations to supervise trajectory planning, which severely limits its scalability. Conversely, although existing perception-free driving world models achieve impressive driving performance, their real-world reasoning ability for planning is solely built on next frame image forecasting. Due to the lack of enough supervision, these models often struggle with comprehensive scene understanding, resulting in unsatisfactory trajectory planning. In this paper, we propose EponaV2, a novel paradigm of driving world models, which achieves high-quality planning with comprehensive future reasoning. Inspired by how human drivers anticipate 3D geometry and semantics, we train our model to forecast more comprehensive future representations, which can be additionally decoded to future geometry and semantic maps. Extracting the 3D and semantic modalities enables our model to deeply understand the surrounding environment, and the future prediction task significantly enhances the real-world reasoning capabilities of EponaV2, ultimately leading to improved trajectory planning. Moreover, inspired by the training recipe of Large Language Models (LLMs), we introduce a flow matching group relative policy optimization mechanism to further improve planning accuracy. The state-of-the-art (SOTA) performances of EponaV2 among perception-free models on three NAVSIM benchmarks (+1.3PDMS, +5.5EPDMS) demonstrate the effectiveness of our methods. <https://github.com/JiaweiXu8/EponaV2>.

1 Introduction

Data scaling laws [27, 88, 12] have proven highly effective in developing neural networks with general intelligence. However, autonomous driving models, which must make trajectory planning decisions across a wide variety of scenarios, still suffer from the high costs associated with training data production. The primary challenge in scaling training data is the expense of manual perception annotations, such as object bounding boxes and semantic segmentations, which are crucial for perception-based models utilizing the popular perception-planning paradigm. Recently, driving models that rely on these manual labels have seen significant improvements in both Bird’s-Eye-View (BEV) methods [22, 26, 56, 37, 35, 41, 78, 48, 72, 46] and Vision-Language-Model (VLM) [70, 15, 98, 38, 71, 47, 55, 32] based approaches. Nevertheless, these methods typically depend on manual annotations to design auxiliary tasks, such as Occupancy Prediction (Occ-Pred) and Visual Question Answering (VQA), to build their perception capabilities. This heavy reliance on expensive manual labeling makes it difficult to apply data scaling laws to perception-based driving models, limiting their potential for stronger planning abilities.

Consequently, perception-free models have been introduced to eliminate the need for manual perception labels during training [9, 3, 96, 92, 36, 95, 77]. However, lacking manual perception supervision,

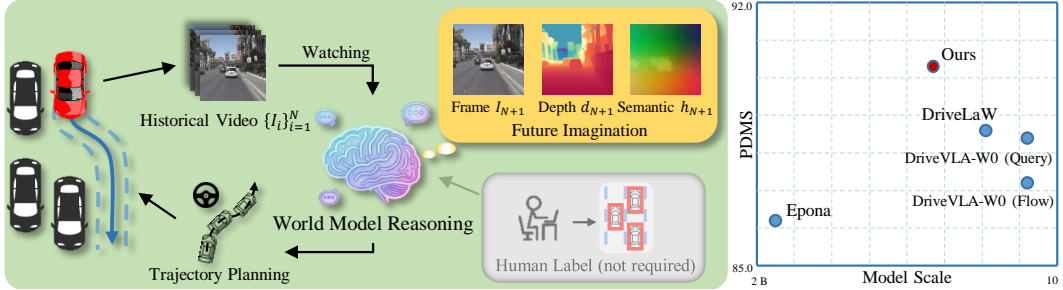


Figure 1: EponaV2. Without relying on manual perception labels, our model develops a strong future reasoning ability of real-world environments for trajectory planning via comprehensive future predictions, achieving SOTA planning performance among perception-free driving world models.

these models often struggle to fully comprehend complex real-world environments. To address this, training world models to reason the representations of the future from current observations for trajectory planning has proven effective for trajectory planning [92, 36, 95, 77]. Naturally, future representations that encode richer and more actionable information require a stronger understanding and reasoning ability of the world and are crucial for better planning. As illustrated in Figure 2, a prevailing method to facilitate future reasoning is to train models to forecast the next video frame [92, 36, 95, 77]. This raises a critical question: *Is the future reasoning ability built solely via next-frame image prediction sufficient for trajectory planning?* We argue that it is insufficient. The information critical for planning within raw images is highly entangled and difficult to utilize directly. Therefore, inferred representations supervised purely by image prediction inherit these ambiguities, posing challenges for better future reasoning ability and trajectory planning.

To address these limitations, we propose EponaV2, a novel paradigm of perception-free driving world models. Inspired by human driving behavior, where decisions rely on anticipating the distances to forward obstacles and understanding their semantic context, we posit that future reasoning for trajectory planning should also utilize both the 3D geometry and semantic information of the environment. To this end, we introduce a simple yet effective perception-free mechanism: the prediction of future depth and semantic maps. By enforcing future depth prediction, EponaV2 comprehensively captures the 3D geometry and motion dynamics of surrounding objects. Furthermore, forecasting future feature maps derived from large-scale segmentation models [6] imparts a profound semantic understanding of the scene, also ensuring that EponaV2 remains focused on elements critical to driving decisions. Without relying on manual perception labels, the comprehensive forecasting approach builds a strong real-world understanding and future reasoning ability for EponaV2. Consequently, the inferred future representations yield rich and actionable information for trajectory planning, substantially boosting overall driving performance. Moreover, inspired by the training recipe of LLMs, we introduce a flow matching Group Relative Policy Optimization (GRPO) mechanism for our flow-based planner to further improve the accuracy of the generated trajectories. This flow matching GRPO autonomously refines the model’s planning results using streamlined reward functions. Experiments on three NAVSIM [5, 11] benchmarks demonstrate that EponaV2 achieves SOTA performance among perception-free driving models, confirming the effectiveness of our approach.

In general, the main contributions of this paper can be summarized as follows.

- We propose EponaV2, a novel perception-free paradigm of driving world models, which achieves high-quality planning and is much easier to perform data scaling training.
- We introduce a novel approach that requires EponaV2 to predict future depth and semantic maps, enabling a stronger future reasoning ability for improved planning.
- We design the flow matching group related policy optimization mechanism to improve the accuracy of the trajectories from our flow matching planner with simple reward functions.

2 Related Work

Perception-Based Driving Models. Perception labels are fundamental to modern perception-planning autonomous driving paradigm, as they enable models to detect and segment surrounding

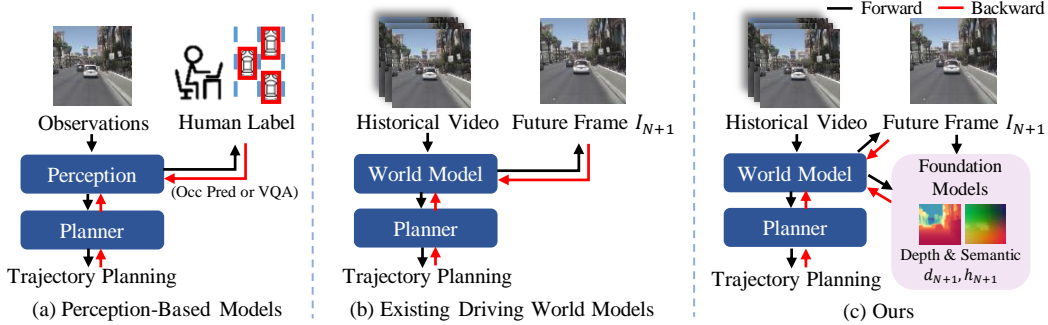


Figure 2: Training Pipeline Comparison. (a) Perception-based models require manual labels to build perception abilities for planning. (b) Existing perception-free driving world models employ limited future trajectory reasoning for planning only by future frame prediction. (c) Ours utilizes foundation models for comprehensive future reasoning by future depth and semantic predictions for better planning.

objects for more effective planning. BEVFormer [40] designs the BEV representation for autonomous driving tasks [22, 26, 8, 67, 56, 10, 63, 37, 35, 28, 68, 44, 39, 90, 23, 83, 54, 49, 94, 91, 25, 97, 46, 18], which aggregates spatial positions and semantic information from the driving environment. Building on this, DiffusionDrive [41, 99] demonstrates that diffusion models [20, 62] serve as powerful policy makers for BEV-based planning. GoalFlow [78] teaches models to predict the goal points for more accurate trajectory generation. BridgeDrive [48] proposes an anchor-guided diffusion bridge policy for closed-loop planning. MeanFuser [72] introduces Gaussian mixture noise to guide trajectory generation for anchor-free planning. SafeDrive [29] performs explicit and interpretable safety reasoning to enable safer and more accurate trajectory generation. For computational efficiency, SparseDrive [65, 89, 16, 85] designs a BEV-free paradigm, while BridgeAD [89] enables the effective use of historical prediction and planning to improve the coherence and accuracy of the models. Research has also explored environmental understanding and scalability; DriveDreamer [73] focuses on real-world comprehension, DrivoR [30] utilizes pretrained Vision Transformers (ViT) with sensor-aware register tokens, and both RAP [14] and SimScale [69] propose scalable data augmentation pipelines. Recently, the success of VLMs has proven their abilities for different tasks [2], and fine-tuning VLMs to Vision-Language-Action (VLA) models for autonomous driving tasks might be a possible way [70, 15, 7, 34, 86, 64, 51, 31, 87, 60, 19, 47, 55, 32, 33, 93, 74, 52, 82, 79, 66]. Notable examples include AutoVLA [98], ReCogDrive [38], and AutoDrive-P³ [84], which perceive environments via a question-and-answer format and improve planning through DPPO [57]. Furthermore, VGGDrive [71] integrates 3D-aware models to enhance the geometric perception of VLA frameworks. Despite these advancements, perception-based models rely heavily on labor-intensive annotations, which hinders their ability to scale with massive datasets.

Perception-Free Driving Models. Unlike perception-based approaches, perception-free models eliminate the need for costly manual labels such as object bounding boxes or semantic segmentation. DrivingGPT [9] employs VLMs to unify simulation and planning tasks, while RoboTron-Sim [3] enhances safety using scenario-aware prompts and an image-to-ego encoder. To facilitate planning without explicit perception, World4Drive [96] constructs a latent world model, and Epona [92] utilizes a diffusion world model for autoregressive video generation. Additionally, DriveVLA-WO [36], DriveLaW [77] and PWM [95] implement dense self-supervision for planning by training on future image predictions. While perception-free models offer advantages in data scaling, they often struggle to interpret complex environments with the limited self-supervision, which can lead to suboptimal performance.

3 Methods

3.1 Applying World Model to Driving with Flow Matching

Input and World Model Backbone. Following the previous works [92], our EponaV2 only takes N frame front-view observation videos $\{I_i\}_{i=1}^N$ and the corresponding relative movements $\{\Delta A_i\}_{i=1}^N$ as input. A strong auto-encoder can effectively extract the semantic information of an image, significantly enhancing the understanding ability of a driving world model. Therefore, we first encode

the images into feature sequences $\{F_i\}_{i=1}^N$ independently using the frozen pretrained DINO-based representation model DINO-Tok [61, 24]. Subsequently, in line with recent approaches [36, 75, 13, 95, 77], we initialize the backbone of our world model with VLMs [2]. By processing these flattened features alongside their associated actions, the backbone implicitly infers the corresponding future representations $\{F'_i, \Delta A'_i\}_{i=1}^N$ for comprehensive world modeling:

$$\{F'_1, \Delta A'_1, F'_2, \Delta A'_2, \dots, F'_N, \Delta A'_N\} = WM(\{F_1, \Delta A_1, F_2, \Delta A_2, \dots, F_N, \Delta A_N\}). \quad (1)$$

During processing, a causal attention mask is applied to the backbone to ensure that future observation features do not influence the current frame inference.

Rectified Flow Matching Planner. Once inferred by the world model backbone, the frame-wise future representations $\{F'_i, \Delta A'_i\}$ are passed to a rectified flow matching [1, 43, 50, 59, 58] planner for trajectory generation. Similar to [92, 78], the flow matching planner v_{traj} predicts the velocity from data samples \mathbf{x}_0 to Gaussian noises $\mathbf{x}_1 \sim \mathcal{N}(\mathbf{0}, \mathbf{I})$:

$$d\mathbf{x}_t = v_{traj}(F'_i, \Delta A'_i, \mathbf{x}_t, t)dt, t \in [0, 1]. \quad (2)$$

During training, the process of adding noise to a data sample for the diffuse timestep t is:

$$\mathbf{x}_t = (1 - t)\mathbf{x}_0 + t\mathbf{x}_1, t \in [0, 1]. \quad (3)$$

To train the flow matching planner, the planner prediction can be supervised by the direction from the ground-truth trajectory to the noise:

$$L_{traj} = \|v_{traj}(F'_i, \Delta A'_i, \mathbf{x}_t, t) - (\mathbf{x}_1 - \mathbf{x}_0)\|^2. \quad (4)$$

Consequently, to derive the predicted trajectory $\hat{\mathbf{x}}_0$, the sampling process for the flow matching planner at each frame is defined as:

$$\hat{\mathbf{x}}_{t+\Delta t} = \hat{\mathbf{x}}_t + v_{traj}(F'_i, \Delta A'_i, \hat{\mathbf{x}}_t, t)\Delta t, t \in [0, 1], \hat{\mathbf{x}}_1 \sim \mathcal{N}(\mathbf{0}, \mathbf{I}). \quad (5)$$

Rectified flow matching planners [92, 78] typically converge much faster than traditional diffusion-based alternatives [62, 20, 38, 41, 99], resulting in a more efficient and streamlined training process.

Rectified Flow Matching Future Frame Predictor. Decoding future representations into the next frame for supervision has proven effective in enabling world models to infer the dynamics of surrounding moving objects, thereby enhancing trajectory planning [92, 36, 95, 77]. Therefore, to establish a coarse world model, following Epona [92], we also perform the next frame prediction of encoded images. Specifically, we employ a rectified flow matching head v_{img} conditioned on the inferred future representation $\{F'_i, \Delta A'_i\}$ and a controlling relative movement ΔA_{i+1} :

$$L_{img} = \|v_{img}(F'_i, \Delta A'_i, \Delta A_{i+1}, t, F_{i+1}^t) - (\epsilon - F_{i+1})\|^2, \\ F_{i+1}^t = (1 - t)F_{i+1} + t\epsilon, t \in [0, 1], \epsilon \sim \mathcal{N}(\mathbf{0}, \mathbf{I}). \quad (6)$$

During inference, the controlling relative movement ΔA_{i+1} , which is supplied as ground truth during training, is instead autonomously predicted by our trajectory planner.

3.2 Forecasting to Reason the Real World

Without the explicit guidance of manual perception labels during training, perception-free driving world models often struggle to fully comprehend complex physical environments. Consequently, future representations inferred by these models frequently lack the rich information necessary for robust trajectory planning. Existing methods [36, 92, 95, 77] typically address this limitation by only decoding the predicted future states into the next video frame for supervision. However, we argue that relying solely on next-frame prediction is inadequate for the complexities of autonomous driving, as the visual information within raw images remains highly entangled and difficult to utilize directly. Besides, critical decision making for both humans and autonomous systems also demands a robust understanding and proactive forecasting of 3D geometry and object semantics. To bridge this gap, we propose two straightforward yet effective training methods that enable the model to reason future by considering these environmental cues without relying on manual annotations.

Reasoning 3D Geometry by Predicting the Future. Accurate 3D geometry encapsulates the spatial position and structural shape of surrounding objects, serving as a critical prerequisite for the safe navigation of autonomous driving models. A prevalent approach to incorporating this 3D context is

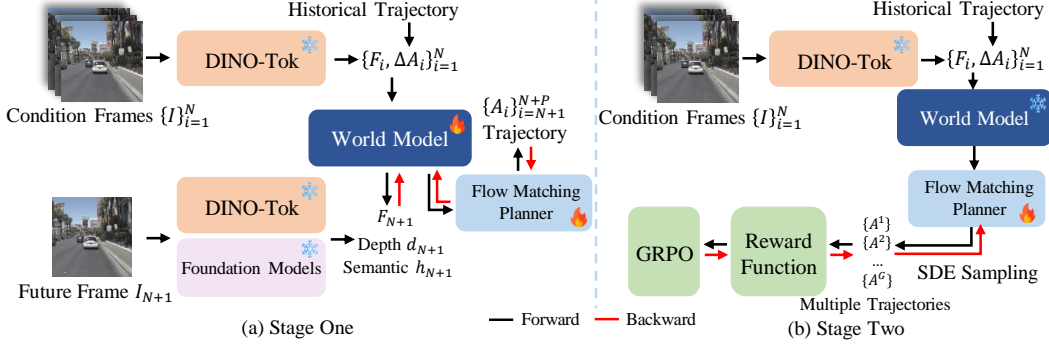


Figure 3: The pipeline of EponaV2. Our model utilizes video sequences encoded by DINO-Tok [24, 61] and corresponding historical trajectories as input. The driving world model reasons the future representations and the trajectory planner decodes these representations into trajectories. (a) For stage one, to build the strong and comprehensive future reasoning ability of EponaV2, we supervise the future image, depth and semantic maps decoded from the inferred future representations with visual foundation models. (b) For stage two, EponaV2 finetunes the predicted trajectory by flow matching GRPO [45] with several simple reward functions.

to supply the driving model with feature representations or outputs derived from pretrained depth estimation networks as additional inputs [71, 96]. However, relying on these auxiliary models for depth-aware inputs introduces extra computational overhead, which inevitably increases the overall trajectory inference latency of the system. Furthermore, without explicitly enforcing the utilization of these depth-aware inputs through task-specific constraints, it remains ambiguous whether the driving model genuinely internalizes these 3D features to infer the future for its planning decisions. To address these concerns, we task our model with predicting the next frame metric depth \hat{d}_{i+1} and a corresponding confidence map \hat{c}_{i+1} . This is achieved by decoding the inferred future representations F'_i to metric depth maps through a lightweight depth head f_d :

$$\{\hat{d}_{i+1}, \hat{c}_{i+1}\} = f_d(F'_i, \Delta \hat{A}_{i+1}), \quad (7)$$

where $\Delta \hat{A}_{i+1}$ represents the controlling relative movement predicted by our flow matching planner. To supervise the depth decoder, we adopt a framework inspired by the visual foundation model Depth-Anything-V3 [80, 81, 42]:

$$L_d = \hat{c}_{i+1} \|\hat{d}_{i+1} - \mathbf{d}_{i+1}\|_1 - \lambda_c \log \hat{c}_{i+1} + \|\nabla_x \hat{d}_{i+1} - \nabla_x \mathbf{d}_{i+1}\|_1 + \|\nabla_y \hat{d}_{i+1} - \nabla_y \mathbf{d}_{i+1}\|_1. \quad (8)$$

In this formulation, \mathbf{d}_{i+1} serves as a pseudo metric depth label for the next frame, generated by Depth-Anything-V3 [42]. Following Metric3D [76, 21], we scale the metric depth using a canonical focal length. This loss allows our model to fully consider the 3D structures and object movements during future reasoning, ultimately enhancing planning performance without incurring extra computational costs during trajectory inference.

Reasoning Semantic Information by Predicting the Future. Another critical factor for effective decision making is the semantic understanding of surrounding objects. While pretrained visual foundation models for segmentation [6] can extract rich semantic information from visual inputs, previous works [96] typically supervise the image backbone via an auxiliary current-frame segmentation task. This approach captures limited semantic context and struggles to explicitly force the driving model to utilize this understanding for future inference and trajectory planning. Therefore, to empower our model to autonomously internalize these semantics, we introduce a novel formulation that explicitly predicts the future-frame feature maps generated by SAM3 [6]. Given an object description, we obtain the encoded text features \mathbf{h}_{text} from the SAM3 text branch and the corresponding text-fused image features \mathbf{h}_i . Similar to our depth module, we utilize a lightweight head f_{sam} to extract the text-aligned feature $\hat{\mathbf{h}}_{i+1}$ for the next frame from the inferred future representation F'_i with the text feature \mathbf{h}_{text} from the text branch of SAM3:

$$\hat{\mathbf{h}}_{i+1} = f_{sam}(F'_i, \Delta \hat{A}_{i+1}, \mathbf{h}_{text}). \quad (9)$$

To facilitate semantic reasoning, we design the following loss function:

$$L_s = \|\hat{\mathbf{h}}_{i+1} - \mathbf{h}_{i+1}\|^2. \quad (10)$$

In this equation, $\hat{\mathbf{h}}_{i+1}$ represents the pseudo next frame feature label generated by SAM3, fused by the text prompt \mathbf{h}_{text} through the SAM3 text encoder. Additionally, by formulating specific text descriptions for various objects in the driving environment, we can direct the attention of our model toward these critical elements. This results in stronger real-world reasoning capabilities and richer future states information for trajectory planning. To achieve faster convergence during training, we replace the predicted controlling movement $\Delta\hat{A}_{i+1}$ in both the depth and semantic branches with the ground truth movement.

3.3 Flow Matching Group Relative Policy Optimization for Planner

Recent studies have demonstrated that reinforcement learning (RL) techniques are highly effective in enhancing the performance of large models, including planning accuracy [98, 38]. To further augment the planning capabilities of our model, we incorporate GRPO into our flow matching planner. Following the Flow-GRPO framework [45], we reformulate the sampling process of the flow matching model as a Stochastic Differential Equation (SDE):

$$\hat{\mathbf{x}}_{t+\Delta t} = \underbrace{\hat{\mathbf{x}}_t \left(1 + \frac{\sigma_t^2}{2t} \Delta t\right) + v_{traj}(F'_i, \Delta A'_i, \hat{\mathbf{x}}_t, t) \cdot \left(1 + \frac{\sigma_t^2(1-t)}{2t}\right) \Delta t}_{\mu_\theta(\hat{\mathbf{x}}_t, t)} + \sigma_t \sqrt{|\Delta t|} \epsilon, \quad \epsilon \sim \mathcal{N}(\mathbf{0}, \mathbf{I}), \quad (11)$$

where $\sigma_t = a\sqrt{\frac{t}{1-t}}$, and a is a scalar hyper-parameter controlling the noise level. In this formulation, the entire diffusion sampling process can be viewed as a continuous decision process [57], where each diffusion step represents a Gaussian policy $\pi_\theta(\hat{\mathbf{x}}_{t+\Delta t}|\hat{\mathbf{x}}_t) = \mathcal{N}(\mu_\theta(\hat{\mathbf{x}}_t, t), \sigma_t^2|\Delta t\mathbf{I})$. After generating a group of trajectory $\{\hat{\mathbf{x}}_0^g\}_{g=1}^G$ using Equation 11, we can compute the group-standardized advantage for each trajectory:

$$A_g = \frac{r_g - \text{mean}(\{r_g\}_{g=1}^G)}{\text{std}(\{r_g\}_{g=1}^G)}, \quad (12)$$

where r_g is the reward of the trajectory $\hat{\mathbf{x}}_0^g$. Directly utilizing PDMS as the reward is unsuitable, as calculating PDMS requires manual perception labels [38, 98]. Therefore, we apply the generated trajectory to control a simulated vehicle, defining the reward based on the discrepancy between the ground-truth trajectory and the vehicle’s simulated trajectory. The policy loss for the diffusion chain is then formulated as:

$$L_{rl} = -\frac{1}{G} \sum_{g=1}^G \frac{1}{T} \sum_{t=1}^T \gamma^{t-1} \log \pi_\theta(\hat{\mathbf{x}}_{(t-1)}^g | \hat{\mathbf{x}}_{(t)}^g) A_g, \quad (13)$$

where γ is the discount factor, T is the total number of diffusion steps, and $\hat{\mathbf{x}}_{(t)}^g$ is the decision at each diffusion step for each group. To stabilize the reinforcement learning process, we introduce an imitation learning loss to regularize the output of our flow matching planner:

$$L_{il} = \|v_{traj}(F'_i, \Delta A'_i, \hat{\mathbf{x}}_t, t) - \frac{\hat{\mathbf{x}}_t - \mathbf{x}_0}{t}\|^2, \quad (14)$$

where \mathbf{x}_0 is the ground truth trajectory. This imitation loss constrains our planner to replicate the ground-truth trajectories from the dataset. Overall, the final GRPO loss is defined as $L_{grpo} = L_{rl} + \lambda_{il}L_{il}$.

Optimization. The optimization of EponaV2 proceeds in two stages. In the first stage, we focus on establishing the model’s future reasoning ability of the real-world environment. Specifically, we freeze the pretrained DINO-Tok and optimize the world model backbone, the depth head f_d , the semantic feature head f_{sam} , and the rectified flow matching heads v_{traj}, v_{img} . The objective function for this first stage is formulated as $L = L_{traj} + L_{img} + L_d + L_s$. In the second stage, we focus on fine-tuning the trajectory planner to achieve higher planning accuracy. To this end, we freeze all components of the model except for the rectified flow matching planner v_{traj} , which is then fine-tuned using the GRPO loss L_{grpo} . The pipeline of EponaV2 is illustrated in Figure 3.

Table 1: Comparison on the NAVSIMv1 [5] benchmark. ‘1xCam’ means the front-view camera. ‘NxCam’ means the surrounding-view cameras. ‘L’ means Lidar.

Method	Perception	Input	NC	DAC	EP	TTC	C	PDMS
Human	-	-	100	100	87.5	100	99.9	94.8
Tranfuser [56]	✓	3xCam + L	97.7	92.8	79.2	92.8	100	84.0
DiffusionDrive [41]	✓	3xCam + L	98.2	96.2	82.2	94.7	100	88.1
VGGDrive [71]	✓	3xCam	98.6	96.3	82.9	95.6	100	88.8
ResWorld [91]	✓	6xCam + L	98.9	96.5	83.1	95.6	100	89.0
MeanFuser [72]	✓	3xCam	98.6	97.0	82.8	95.0	100	89.0
AutoVLA [98]	✓	3x Cam	98.4	95.6	81.9	98.0	99.9	89.1
DriveVLA-W0 (Anchor) [36]	✓	1xCam	98.7	99.1	83.3	95.3	99.3	90.2
AutoDrive-P ³ [84]	✓	3xCam	99.1	97.4	84.8	96.5	100	90.6
ReCogDrive [38]	✓	1xCam	97.9	97.3	87.3	94.9	100	90.8
SafeDrive [29]	✓	3xCam + L	99.5	99.0	84.3	97.2	100	91.6
DrivingGPT [9]		1xCam	98.9	90.7	79.7	94.9	95.6	82.4
World4Drive [96]		3xCam	97.4	94.3	79.9	92.8	100	85.1
Epona [92]		1xCam	97.9	95.1	80.4	93.8	99.9	86.2
DriveVLA-W0 (Flow) [36]		1xCam	98.4	95.3	80.9	95.2	100	87.2
PWM [95]		1xCam	98.6	95.9	81.8	95.4	100	88.1
DriveVLA-W0 (Query) [36]		1xCam	98.7	96.2	82.2	95.5	100	88.4
DriveLaW [77]		1xCam	99.0	97.1	81.3	96.7	100	89.1
EponaV2 (Ours)		1xCam	98.6	97.9	84.8	95.7	100	90.4

Table 2: Comparison on the NAVSIMv2 [11] (navhard split) benchmark with human penalty **enabled**.

Method	Perception	Stage	NC	DAC	DDC	TLC	EP	TTC	LK	HC	EC	EPDMS
LTF [10]	✓	1	96.2	79.6	99.1	99.6	84.1	95.1	94.2	97.6	79.1	25.1
		2	77.8	70.2	84.3	98.1	85.1	75.7	45.4	95.7	76.0	
LTFv6 [53]	✓	1	96.6	86.7	99.2	99.6	84.5	95.1	94.4	97.8	76.4	31.9
		2	79.9	75.6	86.3	97.9	89.6	76.1	50.1	95.2	66.7	
RAP [14]	✓	1	97.1	94.4	98.8	99.8	83.9	96.9	94.7	96.4	66.2	39.6
		2	83.2	83.9	87.4	98.0	86.9	80.4	52.3	95.2	52.4	
DriveVLA-W0 [36]		1	96.8	83.3	99.0	99.6	84.6	95.3	96.4	97.6	78.2	24.4
		2	76.8	64.3	79.9	98.3	89.2	75.0	46.8	95.8	53.1	
DriveLaW [77]		1	97.3	89.1	99.2	99.6	84.3	97.1	96.2	97.8	67.6	30.6
		2	82.5	67.6	83.5	98.1	84.8	78.5	45.8	96.4	57.3	
EponaV2 (Ours)		1	97.3	90.7	99.4	100	83.3	97.3	97.3	97.6	60.9	36.1
		2	83.6	78.0	88.0	98.9	86.0	80.3	50.1	96.1	52.0	

4 Experiments

4.1 Setup

Benchmarks. To evaluate our model, we select three challenging benchmarks from the NAVSIM [5, 11] dataset: the ‘navtest’ split evaluated under NAVSIMv1 metrics, the ‘navtest’ split under NAVSIMv2 metrics, and the ‘navhard’ split under NAVSIMv2 metrics. The primary metric for NAVSIMv1 [5] is PDMS, which comprehensively assesses the model’s performance across several dimensions: no at-fault collision (NC), drivable area compliance (DAC), ego progress (EP), time-to-collision (TTC) and comfort (C). The primary metric for NAVSIMv2 [11] is EPDMS. In addition to the base PDMS components, EPDMS incorporates traffic light compliance (TLC) and lane keeping (LK), while expanding comfort (C) into history comfort (HC) and extended comfort (EC). For all reported metrics, higher values indicate better performance.

Table 3: Comparison on the NAVSIMv2 [11] (navtest split) benchmark with human penalty **enabled**.

Method	Perception	NC	DAC	DDC	TLC	EP	TTC	LK	HC	EC	EPDMS
Human	-	100	100	99.8	100	87.4	199	199	98.1	90.1	94.5
Tranfuser [56]	✓	96.9	89.9	97.8	99.7	87.1	95.4	92.7	98.3	87.2	84.0
WoTE [37]	✓	98.5	96.8	98.8	99.8	86.1	97.9	95.5	98.3	82.9	87.7
DiffusionDrive [41]	✓	98.2	96.2	99.5	99.8	87.4	97.3	96.9	98.4	87.7	88.2
AutoDrive-P ³ [84]	✓	99.1	97.4	99.2	99.8	88.0	98.7	96.3	98.3	85.5	89.9
DriveVLA-W0 [36]		98.4	95.2	99.4	99.9	86.6	97.9	97.8	98.3	82.7	86.9
PWM [95]		98.8	95.9	99.4	99.9	86.4	98.4	97.6	98.3	85.3	88.2
DriveLaW [77]		98.7	96.9	99.6	99.8	87.5	98.3	97.6	98.4	77.4	88.6
EponaV2 (Ours)		98.5	97.4	99.5	99.9	87.9	98.1	97.7	98.2	77.4	88.9

Table 4: Ablation of the future prediction on the NAVSIMv1 [5] benchmark. The models are downscaled by using Qwen3-VL [2] 2B as the world model backbone.

L_{traj}	L_{img}	L_d	L_s	NC	DAC	EP	TTC	C	PDMS
✓				97.0	94.5	79.7	91.5	99.9	84.4
✓	✓			96.6	95.4	79.9	91.2	99.9	84.8
✓		✓		97.3	95.0	79.4	93.2	99.9	85.2
✓	✓	✓		97.1	95.4	80.6	92.3	99.9	85.6
✓	✓	✓	✓	97.7	96.1	81.4	93.5	100	86.9

Implementation. We adopt the language part of Qwen3-VL 4B [2] to initialize our world model backbone. Totally, EponaV2 has 6.7B parameters. The input video resolution and frame rate are set to 512×1024 and 2Hz respectively. The text features h_{text} in Equation 9 are extracted via the SAM3 [6] text encoder using ‘car’ and ‘human’ as prompts. The entire training process requires approximately 10 days and is distributed across 64 H20 GPUs. During the first stage, we train EponaV2 on the nuPlan [17] and nuScenes [4] datasets using 5-frame video clips to establish the model’s foundational future reasoning ability of the real world. In the second stage, we exclusively finetune the trajectory planner on the ‘navtrain’ split of the NAVSIM dataset, utilizing navigational commands and 4-frame video inputs. This stage incorporates our proposed flow matching GRPO to further enhance planning accuracy. The evaluation of our model is conducted on a single RTX 4090 GPU.

4.2 Comparison

Comparison on the NAVSIMv1 [5] Benchmark. Table 1 presents a comparison of our model with SOTA perception-based and perception-free models. We classify DriveVLA-W0 (Anchor) [36] as a perception-based model because it applies manual perception labels to PDMS calculation for each trajectory anchor and uses the PDMS results to choose trajectories for supervision. As shown in Table 1, despite not relying on any manual perception labels, our model achieves planning performance comparable to that of perception-based models. Compared to other perception-free models, our model significantly outperforms Drive-VLA-W0 [36] and DriveLaW [77], achieving a notable **+1.3** improvement in PDMS. These results demonstrate that incorporating future depth and semantic predictions, along with fine-tuning via flow matching GRPO, empowers driving models to better understand the environment and enables the planner to generate more accurate trajectories.

Comparison on the NAVSIMv2 [11] Benchmark. The NAVSIMv2 [11] benchmark employs a two-stage pseudo closed-loop evaluation. The corresponding results are presented in Table 3 and Table 2. For a fair comparison, we additionally evaluate DriveVLA-W0 (Flow) [36], PWM [95] and DriveLaW [77] on these benchmarks using their publicly available checkpoints. EponaV2 achieves superior performance than other perception-free models on these more challenging benchmarks, which feature longer simulation horizons. Notably, on the ‘navhard’ split of NAVSIMv2 benchmark, our model has **+5.5** improvement in EPDMS. The higher EPDMS underscores our model’s robust reasoning capabilities across diverse driving scenarios.

Table 5: Comparison of predicting the future and the present on the NAVSIMv1 [5] Benchmark. The models are downscaled by using Qwen3-VL [2] 2B as the world model backbone and only have the depth predictor for self-supervision.

Prediction	NC	DAC	EP	TTC	C	PDMS
Present Frame	96.3	94.5	78.8	90.8	99.8	83.6
Future Frame	97.3	95.0	79.4	93.2	99.9	85.2

Table 6: Ablation of the flow matching GRPO on the NAVSIMv1 [5] Benchmark.

Model	NC	DAC	EP	TTC	C	PDMS
EponaV2 w/o L_{grpo}	98.6	97.3	83.6	95.3	99.9	89.4
EponaV2 (Ours)	98.6	97.9	84.8	95.7	100	90.4

4.3 Ablation Study

Ablation of Future Prediction Losses. The prediction losses task the model with forecasting future depth, images, and SAM3-generated semantic maps [6], thereby establishing the ability of our model to comprehend the real-world environment and predict the future for trajectory planning. Due to the high computational cost associated with training the full-scale model, we conduct an ablation study on these losses by downscaling EponaV2 to 3.5B parameters using the Qwen3-VL [2] 2B as the world model backbone. The results of progressively integrating these prediction losses are presented in Table 4. The results demonstrate that the depth loss enhances the model’s understanding of 3D geometry, yielding notable improvements in NC, DAC and TTC. Furthermore, the semantic map loss facilitates the extraction of semantic information from surrounding objects, which effectively prevents collisions and guides EponaV2 to maintain safe, rule-compliant driving trajectories.

Predict the Present v.s. the Future. The future-forecasting forces EponaV2 to utilize depth and semantic information for better trajectory planning. To further demonstrate its effectiveness, we conduct an experiment comparing the impact of predicting current versus future depth maps. Specifically, the setting ‘Present Frame’ utilizes the current depth map to supervise the model, and the ‘Future Frame’ setting utilizes the future depth map. In both configurations, we rely solely on the depth predictor to establish the model’s real-world reasoning capabilities and downscale our model for faster training. The corresponding results are presented in Table 5. The superior performance achieved by forecasting future frames indicates that this approach fosters a substantially stronger and more comprehensive real-world future reasoning ability for trajectory planning within the model.

Ablation of Flow Matching GRPO. The flow matching GRPO further optimizes the trajectory planner using reinforcement learning techniques. To evaluate its impact, we conduct an ablation study where the GRPO loss L_{grpo} is removed, denoted as the ‘EponaV2 w/o L_{grpo} ’ setting. The results of this ablation study are presented in Table 6. These findings demonstrate that the flow matching GRPO significantly enhances planning accuracy, as evidenced by notable improvements in the EP metric.

5 Conclusion

In this paper, we propose EponaV2, a novel paradigm of a perception-free driving world model. To equip our model with comprehensive real-world future reasoning capabilities, we designed losses that task the model with predicting the depth and semantic maps of future frames. By forecasting this 3D and semantic information, EponaV2 can effectively perceive the geometry of surrounding objects and comprehend their semantic context, resulting in enhanced trajectory planning performance. Additionally, we introduce a flow matching group relative policy optimization mechanism to further refine our trajectory planner and improve overall planning accuracy. Extensive experiments demonstrate the effectiveness of our proposed approach. However, our model does not yet surpass SOTA perception-based models, primarily due to challenges arising from the inherent imprecision of the pseudo depth and semantic labels generated by pretrained foundational models. We leave the resolution of these limitations to future work and we hope that EponaV2 will inspire further exploration into perception-free models toward the realization of true general driving intelligence.

References

- [1] Michael Samuel Albergo and Eric Vanden-Eijnden. Building normalizing flows with stochastic interpolants. In *The Eleventh International Conference on Learning Representations*, 2023.
- [2] Shuai Bai, Yuxuan Cai, Ruizhe Chen, Keqin Chen, Xionghui Chen, Zesen Cheng, Lianghao Deng, Wei Ding, Chang Gao, Chunjiang Ge, Wenbin Ge, Zhifang Guo, Qidong Huang, Jie Huang, Fei Huang, Binyuan Hui, Shutong Jiang, Zhaohai Li, Mingsheng Li, Mei Li, Kaixin Li, Zicheng Lin, Junyang Lin, Xuejing Liu, Jiawei Liu, Chenglong Liu, Yang Liu, Dayiheng Liu, Shixuan Liu, Dunjie Lu, Ruilin Luo, Chenxu Lv, Rui Men, Lingchen Meng, Xuancheng Ren, Xingzhang Ren, Sibao Song, Yuchong Sun, Jun Tang, Jianhong Tu, Jianqiang Wan, Peng Wang, Pengfei Wang, Qiuyue Wang, Yuxuan Wang, Tianbao Xie, Yiheng Xu, Haiyang Xu, Jin Xu, Zhibo Yang, Mingkun Yang, Jianxin Yang, An Yang, Bowen Yu, Fei Zhang, Hang Zhang, Xi Zhang, Bo Zheng, Humen Zhong, Jingren Zhou, Fan Zhou, Jing Zhou, Yuanzhi Zhu, and Ke Zhu. Qwen3-VL technical report. *arXiv preprint arXiv:2511.21631*, 2025.
- [3] Xiao Baihui, Feng Chengjian, Huang Zhijian, Yan Feng, Zhong Yujie, and Ma Lin. RoboTron-Sim: Improving real-world driving via simulated hard-case. *arXiv preprint arXiv:0000.00000*, 2025.
- [4] Holger Caesar, Varun Bankiti, Alex H. Lang, Sourabh Vora, Venice Erin Liong, Qiang Xu, Anush Krishnan, Yu Pan, Giancarlo Baldan, and Oscar Beijbom. NuScenes: A multimodal dataset for autonomous driving. *arXiv preprint arXiv:1903.11027*, 2019.
- [5] Wei Cao, Marcel Hallgarten, Tianyu Li, Daniel Dauner, Xunjiang Gu, Caojun Wang, Yakov Miron, Marco Aiello, Hongyang Li, Igor Gilitschenski, Boris Ivanovic, Marco Pavone, Andreas Geiger, and Kashyap Chitta. Pseudo-simulation for autonomous driving. In *Conference on Robot Learning (CoRL)*, 2025.
- [6] Nicolas Carion, Laura Gustafson, Yuan-Ting Hu, Shoubhik Debnath, Ronghang Hu, Didac Suris, Chaitanya Ryali, Kalyan Vasudev Alwala, Haitham Khedr, Andrew Huang, Jie Lei, Tengyu Ma, Baishan Guo, Arpit Kalla, Markus Marks, Joseph Greer, Meng Wang, Peize Sun, Roman Rädle, Triantafyllos Afouras, Effrosyni Mavroudi, Katherine Xu, Tsung-Han Wu, Yu Zhou, Liliane Momeni, Rishi Hazra, Shuangrui Ding, Sagar Vaze, Francois Porcher, Feng Li, Siyuan Li, Aishwarya Kamath, Ho Kei Cheng, Piotr Dollár, Nikhila Ravi, Kate Saenko, Pengchuan Zhang, and Christoph Feichtenhofer. SAM 3: Segment anything with concepts. *arXiv preprint arXiv:2511.16719*, 2025.
- [7] Canyu Chen, Yuguang Yang, Zhewen Tan, Yizhi Wang, Ruiyi Zhan, Haiyan Liu, Xuanyao Mao, Jason Bao, Xinyue Tang, Linlin Yang, et al. Devil is in narrow policy: Unleashing exploration in driving VLA models. *arXiv preprint arXiv:2603.06049*, 2026.
- [8] Shaoyu Chen, Bo Jiang, Hao Gao, Bencheng Liao, Qing Xu, Qian Zhang, Chang Huang, Wenyu Liu, and Xinggang Wang. VADv2: End-to-end vectorized autonomous driving via probabilistic planning. *arXiv preprint arXiv:2402.13243*, 2024.
- [9] Yuntao Chen, Yuqi Wang, and Zhaoxiang Zhang. DrivingGPT: Unifying driving world modeling and planning with multi-modal autoregressive transformers. In *Proceedings of the IEEE/CVF International Conference on Computer Vision*, pages 26890–26900, 2025.
- [10] Kashyap Chitta, Aditya Prakash, Bernhard Jaeger, Zehao Yu, Katrin Renz, and Andreas Geiger. TransFuser: Imitation with transformer-based sensor fusion for autonomous driving. *IEEE transactions on pattern analysis and machine intelligence*, 45(11):12878–12895, 2022.
- [11] Daniel Dauner, Marcel Hallgarten, Tianyu Li, Xinshuo Weng, Zhiyu Huang, Zetong Yang, Hongyang Li, Igor Gilitschenski, Boris Ivanovic, Marco Pavone, Andreas Geiger, and Kashyap Chitta. NAVSIM: Data-driven non-reactive autonomous vehicle simulation and benchmarking. In *Advances in Neural Information Processing Systems (NeurIPS)*, 2024.
- [12] Mostafa Dehghani, Josip Djolonga, Basil Mustafa, Piotr Padlewski, Jonathan Heek, Justin Gilmer, Andreas Peter Steiner, Mathilde Caron, Robert Geirhos, Ibrahim Alabdulmohsin, et al. Scaling vision transformers to 22 billion parameters. In *International conference on machine learning*, pages 7480–7512. PMLR, 2023.
- [13] Cunxin Fan, Xiaosong Jia, Yihang Sun, Yixiao Wang, Jianglan Wei, Ziyang Gong, Xiangyu Zhao, Masayoshi Tomizuka, Xue Yang, Junchi Yan, and Mingyu Ding. Interleave-VLA: Enhancing robot manipulation with interleaved image-text instructions. *arXiv preprint arXiv:2505.02152*, 2025.
- [14] Lan Feng, Yang Gao, Eloi Zablocki, Quanyi Li, Wuyang Li, Sichao Liu, Matthieu Cord, and Alexandre Alahi. RAP: 3D rasterization augmented end-to-end planning. *arXiv preprint arXiv:2510.04333*, 2025.

- [15] Haoyu Fu, Diankun Zhang, Zongchuang Zhao, Jianfeng Cui, Ding kang Liang, Chong Zhang, Dingyuan Zhang, Hongwei Xie, Bing Wang, and Xiang Bai. ORION: A holistic end-to-end autonomous driving framework by vision-language instructed action generation. In *Proceedings of the IEEE/CVF International Conference on Computer Vision*, 2025.
- [16] Mingzhe Guo, Yixiang Yang, Chuanrong Han, Rufeng Zhang, Shirui Li, Ji Wan, and Zhipeng Zhang. FlowAD: Ego-scene interactive modeling for autonomous driving. *arXiv preprint arXiv:2603.13399*, 2026.
- [17] K. Tan et al. H. Caesar, J. Kabzan. NuPlan: A closed-loop ML-based planning benchmark for autonomous vehicles. In *CVPR ADP3 workshop*, 2021.
- [18] Jianhua Han, Meng Tian, Jiangtong Zhu, Fan He, Huixin Zhang, Sitong Guo, Dechang Zhu, Hao Tang, Pei Xu, Yuze Guo, et al. Percept-WAM: Perception-enhanced world-awareness-action model for robust end-to-end autonomous driving. *arXiv preprint arXiv:2511.19221*, 2025.
- [19] Deepti Hegde, Rajeev Yasarla, Hong Cai, Shizhong Han, Apratim Bhattacharyya, Shweta Mahajan, Litian Liu, Risheek Garrepalli, Vishal M Patel, and Fatih Porikli. Distilling multi-modal large language models for autonomous driving. In *Proceedings of the Computer Vision and Pattern Recognition Conference*, pages 27575–27585, 2025.
- [20] Jonathan Ho, Ajay Jain, and Pieter Abbeel. Denoising diffusion probabilistic models. *Advances in neural information processing systems*, 33:6840–6851, 2020.
- [21] Mu Hu, Wei Yin, Chi Zhang, Zhipeng Cai, Xiaoxiao Long, Hao Chen, Kaixuan Wang, Gang Yu, Chunhua Shen, and Shaojie Shen. Metric3Dv2: A versatile monocular geometric foundation model for zero-shot metric depth and surface normal estimation. *IEEE Transactions on Pattern Analysis and Machine Intelligence*, 2024.
- [22] Yihan Hu, Jiazhi Yang, Li Chen, Keyu Li, Chonghao Sima, Xizhou Zhu, Siqi Chai, Senyao Du, Tianwei Lin, Wenhai Wang, et al. Planning-oriented autonomous driving. In *Proceedings of the IEEE/CVF conference on computer vision and pattern recognition*, pages 17853–17862, 2023.
- [23] Yi Huang, zhan qu, Lihui Jiang, Bingbing Liu, and Hongbo Zhang. Prioritizing perception-guided self-supervision: A new paradigm for causal modeling in end-to-end autonomous driving. In *The Thirty-ninth Annual Conference on Neural Information Processing Systems*, 2025.
- [24] Mingkai Jia, Mingxiao Li, Zhijian Shu, Anlin Zheng, Liaoyuan Fan, Jiabin Guo, Tianxing Shi, Dongyue Lu, Zeming Li, Xiaoyang Guo, Xiaojuan Qi, Xiao-Xiao Long, Qian Zhang, Ping Tan, and Wei Yin. DINO-Tok: Adapting DINO for visual tokenizers. *arXiv preprint arXiv:2511.20565*, 2026.
- [25] Xiaosong Jia, Chenhe Zhang, Yule Jiang, Songbur Wong, Zhiyuan Zhang, Chen Chen, Shaofeng Zhang, Xuanhe Zhou, Xue Yang, Junchi Yan, et al. Spatial retrieval augmented autonomous driving. *arXiv preprint arXiv:2512.06865*, 2025.
- [26] Bo Jiang, Shaoyu Chen, Qing Xu, Bencheng Liao, Jiajie Chen, Helong Zhou, Qian Zhang, Wenyu Liu, Chang Huang, and Xinggang Wang. VAD: Vectorized scene representation for efficient autonomous driving. In *Proceedings of the IEEE/CVF International Conference on Computer Vision*, pages 8340–8350, 2023.
- [27] Jared Kaplan, Sam McCandlish, Tom Henighan, Tom B Brown, Benjamin Chess, Rewon Child, Scott Gray, Alec Radford, Jeffrey Wu, and Dario Amodei. Scaling laws for neural language models. *arXiv preprint arXiv:2001.08361*, 2020.
- [28] Jongsuk Kim, Jaeyoung Lee, Gyojin Han, Dong-Jae Lee, Minki Jeong, and Junmo Kim. SynAD: Enhancing real-world end-to-end autonomous driving models through synthetic data integration. In *Proceedings of the IEEE/CVF International Conference on Computer Vision*, pages 25197–25206, 2025.
- [29] Jungho Kim, Jiyong Oh, Seunghoon Yu, Hongjae Shin, Donghyuk Kwak, and Jun Won Choi. SafeDrive: Fine-grained safety reasoning for end-to-end driving in a sparse world. *arXiv preprint arXiv:2602.18887*, 2026.
- [30] Ellington Kirby, Alexandre Boulch, Yihong Xu, Yuan Yin, Gilles Puy, Éloi Zablocki, Andrei Bursuc, Spyros Gidaris, Renaud Marlet, Florent Bartoccioni, Anh-Quan Cao, Nermin Samet, Tuan-Hung Vu, and Matthieu Cord. Driving on registers. In *CVPR*, 2026.
- [31] Fanjie Kong, Yitong Li, Weihuang Chen, Chen Min, Yizhe Li, Zhiqiang Gao, Haoyang Li, Zhongyu Guo, and Hongbin Sun. VLR-Driver: Large vision-language-reasoning models for embodied autonomous driving. In *Proceedings of the IEEE/CVF International Conference on Computer Vision (ICCV)*, pages 26966–26976, October 2025.

- [32] Jingyu Li, Junjie Wu, Dongnan Hu, Xiangkai Huang, Bin Sun, Zhihui Hao, Xianpeng Lang, Xiatian Zhu, and Li Zhang. SGDrive: Scene-to-goal hierarchical world cognition for autonomous driving. *arXiv preprint arXiv:2601.05640*, 2026.
- [33] Peizheng Li, Zhenghao Zhang, David Holtz, Hang Yu, Yutong Yang, Yuzhi Lai, Rui Song, Andreas Geiger, and Andreas Zell. SpaceDrive: Infusing spatial awareness into VLM-based autonomous driving. *arXiv preprint arXiv:2512.10719*, 2025.
- [34] Pengxiang Li, Yinan Zheng, Yue Wang, Huimin Wang, Hang Zhao, Jingjing Liu, Xianyuan Zhan, Kun Zhan, and Xianpeng Lang. Discrete diffusion for reflective vision-language-action models in autonomous driving. *arXiv preprint arXiv:2509.20109*, 2025.
- [35] Yingyan Li, Lue Fan, Jiawei He, Yuqi Wang, Yuntao Chen, Zhaoxiang Zhang, and Tieniu Tan. Enhancing end-to-end autonomous driving with latent world model. *arXiv preprint arXiv:2406.08481*, 2024.
- [36] Yingyan Li, Shuyao Shang, Weisong Liu, Bing Zhan, Haochen Wang, Yuqi Wang, Yuntao Chen, Xiaoman Wang, Yasong An, Chufeng Tang, et al. DriveVLA-W0: World models amplify data scaling law in autonomous driving. *arXiv preprint arXiv:2510.12796*, 2025.
- [37] Yingyan Li, Yuqi Wang, Yang Liu, Jiawei He, Lue Fan, and Zhaoxiang Zhang. End-to-end driving with online trajectory evaluation via BEV world model. In *Proceedings of the IEEE/CVF International Conference on Computer Vision (ICCV)*, pages 27137–27146, October 2025.
- [38] Yongkang Li, Kaixin Xiong, Xiangyu Guo, Fang Li, Sixu Yan, Gangwei Xu, Lijun Zhou, Long Chen, Haiyang Sun, Bing Wang, et al. ReCogDrive: A reinforced cognitive framework for end-to-end autonomous driving. *arXiv preprint arXiv:2506.08052*, 2025.
- [39] Zhenxin Li, Shihao Wang, Shiyi Lan, Zhiding Yu, Zuxuan Wu, and Jose M. Alvarez. Hydra-NeXt: Robust closed-loop driving with open-loop training. In *Proceedings of the IEEE/CVF International Conference on Computer Vision (ICCV)*, pages 27305–27314, October 2025.
- [40] Zhiqi Li, Wenhao Wang, Hongyang Li, Enze Xie, Chonghao Sima, Tong Lu, Qiao Yu, and Jifeng Dai. BEVFormer: Learning bird’s-eye-view representation from Lidar-camera via spatiotemporal transformers. *IEEE Transactions on Pattern Analysis and Machine Intelligence*, 47(3):2020–2036, 2024.
- [41] Bencheng Liao, Shaoyu Chen, Haoran Yin, Bo Jiang, Cheng Wang, Sixu Yan, Xinbang Zhang, Xiangyu Li, Ying Zhang, Qian Zhang, et al. DiffusionDrive: Truncated diffusion model for end-to-end autonomous driving. In *Proceedings of the Computer Vision and Pattern Recognition Conference*, pages 12037–12047, 2025.
- [42] Haotong Lin, Sili Chen, Jun Hao Liew, Donny Y. Chen, Zhenyu Li, Guang Shi, Jiashi Feng, and Bingyi Kang. Depth anything 3: Recovering the visual space from any views. *arXiv preprint arXiv:2511.10647*, 2025.
- [43] Yaron Lipman, Ricky T. Q. Chen, Heli Ben-Hamu, Maximilian Nickel, and Matthew Le. Flow matching for generative modeling. In *The Eleventh International Conference on Learning Representations*, 2023.
- [44] Changxing Liu, Genjia Liu, Zijun Wang, Jinchang Yang, and Siheng Chen. CoLMDriver: LLM-based negotiation benefits cooperative autonomous driving. *arXiv preprint arXiv:2503.08683*, 2025.
- [45] Jie Liu, Gongye Liu, Jiajun Liang, Yangguang Li, Jiaheng Liu, Xintao Wang, Pengfei Wan, Di Zhang, and Wanli Ouyang. Flow-GRPO: Training flow matching models via online RL. *arXiv preprint arXiv:2505.05470*, 2025.
- [46] Lin Liu, Caiyan Jia, Guanyi Yu, Ziyang Song, JunQiao Li, Feiyang Jia, Peiliang Wu, Xiaoshuai Hao, and Yandan Luo. GuideFlow: Constraint-guided flow matching for planning in end-to-end autonomous driving. *arXiv preprint arXiv:2511.18729*, 2025.
- [47] Pei Liu, Qingtian Ning, Xinyan Lu, Haipeng Liu, Weiliang Ma, Dangen She, Xianpeng Lang, and Jun Ma. CogDriver: Integrating cognitive inertia for temporally coherent planning in autonomous driving. *arXiv preprint arXiv:2509.00789v2*, 2025.
- [48] Shu Liu, Wenlin Chen, Weihao Li, Zheng Wang, Lijin Yang, Jianing Huang, Yipin Zhang, Zhongzhan Huang, Ze Cheng, and Hao Yang. BridgeDrive: Diffusion bridge policy for closed-loop trajectory planning in autonomous driving. *arXiv preprint arXiv:2509.23589*, 2025.
- [49] Shuai Liu, Quanmin Liang, Zefeng Li, Boyang Li, and Kai Huang. GaussianFusion: Gaussian-based multi-sensor fusion for end-to-end autonomous driving. In *The Thirty-ninth Annual Conference on Neural Information Processing Systems*, 2025.

- [50] Xingchao Liu, Chengyue Gong, and qiang liu. Flow straight and fast: Learning to generate and transfer data with rectified flow. In *The Eleventh International Conference on Learning Representations*, 2023.
- [51] Yuhang Lu, Jiadong Tu, Yuexin Ma, and Xinge Zhu. ReAL-AD: Towards human-like reasoning in end-to-end autonomous driving. *arXiv preprint arXiv:2507.12499*, 2025.
- [52] Yuechen Luo, Qimao Chen, Fang Li, Shaoqing Xu, Jaxin Liu, Ziyang Song, Zhi-xin Yang, and Fuxi Wen. Unleashing VLA potentials in autonomous driving via explicit learning from failures. *arXiv preprint arXiv:2603.01063*, 2026.
- [53] Long Nguyen, Micha Fauth, Bernhard Jaeger, Daniel Dauner, Maximilian Igl, Andreas Geiger, and Kashyap Chitta. LEAD: Minimizing learner-expert asymmetry in end-to-end driving. In *Conference on Computer Vision and Pattern Recognition (CVPR)*, 2026.
- [54] Ling Niu, Xiaoji Zheng, han wang, Ziyuan Yang, Chen Zheng, Bokui Chen, and Jiangtao Gong. Embodied cognition augmented end2end autonomous driving. In *The Thirty-ninth Annual Conference on Neural Information Processing Systems*, 2025.
- [55] Qihang Peng, Xuesong Chen, Chenye Yang, Shaoshuai Shi, and Hongsheng Li. ColaVLA: Leveraging cognitive latent reasoning for hierarchical parallel trajectory planning in autonomous driving. *arXiv preprint arXiv:2512.22939*, 2025.
- [56] Aditya Prakash, Kashyap Chitta, and Andreas Geiger. Multi-modal fusion transformer for end-to-end autonomous driving. In *Proceedings of the IEEE/CVF conference on computer vision and pattern recognition*, pages 7077–7087, 2021.
- [57] Allen Z Ren, Justin Lidard, Lars L Ankile, Anthony Simeonov, Pulkit Agrawal, Anirudha Majumdar, Benjamin Burchfiel, Hongkai Dai, and Max Simchowitz. Diffusion policy policy optimization. *arXiv preprint arXiv:2409.00588*, 2024.
- [58] Minglei Shi, Haolin Wang, Borui Zhang, Wenzhao Zheng, Bohan Zeng, Ziyang Yuan, Xiaoshi Wu, Yuanxing Zhang, Huan Yang, Xintao Wang, Pengfei Wan, Kun Gai, Jie Zhou, and Jiwen Lu. SVG-T2I: Scaling up text-to-image latent diffusion model without variational autoencoder. *arXiv preprint arXiv:2512.11749*, 2025.
- [59] Minglei Shi, Haolin Wang, Wenzhao Zheng, Ziyang Yuan, Xiaoshi Wu, Xintao Wang, Pengfei Wan, Jie Zhou, and Jiwen Lu. Latent diffusion model without variational autoencoder. *arXiv preprint arXiv:2510.15301*, 2025.
- [60] Chonghao Sima, Katrin Renz, Kashyap Chitta, Li Chen, Hanxue Zhang, Chengen Xie, Ping Luo, Andreas Geiger, and Hongyang Li. DriveLM: Driving with graph visual question answering. *arXiv preprint arXiv:2312.14150*, 2023.
- [61] Oriane Siméoni, Huy V. Vo, Maximilian Seitzer, Federico Baldassarre, Maxime Oquab, Cijo Jose, Vasil Khalidov, Marc Szafraniec, Seungeun Yi, Michaël Ramamonjisoa, Francisco Massa, Daniel Haziza, Luca Wehrstedt, Jianyuan Wang, Timothée Darcet, Théo Moutakanni, Leonel Sentana, Claire Roberts, Andrea Vedaldi, Jamie Tolan, John Brandt, Camille Couprie, Julien Mairal, Hervé Jégou, Patrick Labatut, and Piotr Bojanowski. DINOv3. *arXiv preprint arXiv:2508.10104*, 2025.
- [62] Jiaming Song, Chenlin Meng, and Stefano Ermon. Denoising diffusion implicit models. *arXiv preprint arXiv:2010.02502*, 2020.
- [63] Ziyang Song, Caiyan Jia, Lin Liu, Hongyu Pan, Yongchang Zhang, Junming Wang, Xingyu Zhang, Shaoqing Xu, Lei Yang, and Yadan Luo. Don’t shake the wheel: Momentum-aware planning in end-to-end autonomous driving. In *Proceedings of the IEEE/CVF Conference on Computer Vision and Pattern Recognition*, pages 22432–22441, 2025.
- [64] Haisheng Su, Wei Wu, Feixiang Song, Junjie Zhang, Zhenjie Yang, and Junchi Yan. DriveMamba: Task-centric scalable state space model for efficient end-to-end autonomous driving. In *The Fourteenth International Conference on Learning Representations*, 2026.
- [65] Wenchao Sun, Xuewu Lin, Yining Shi, Chuang Zhang, Haoran Wu, and Sifa Zheng. SparseDrive: End-to-end autonomous driving via sparse scene representation. In *2025 IEEE International Conference on Robotics and Automation (ICRA)*, pages 8795–8801. IEEE, 2025.
- [66] Shuhan Tan, Kashyap Chitta, Yuxiao Chen, Ran Tian, Yurong You, Yan Wang, Wenjie Luo, Yulong Cao, Philipp Krahenbuhl, Marco Pavone, and Boris Ivanovic. Latent chain-of-thought world modeling for end-to-end driving. *arXiv preprint arXiv:2512.10226*, 2026.

- [67] Jiacheng Tang, Zhiyuan Zhou, Zhuolin He, Jia Zhang, Kai Zhang, and Jian Pu. CausalVAD: Deconfounding end-to-end autonomous driving via causal intervention. *arXiv preprint arXiv:2603.18561*, 2026.
- [68] Yingqi Tang, Zhuoran Xu, Zhaotie Meng, and Erkang Cheng. HiP-AD: Hierarchical and multi-granularity planning with deformable attention for autonomous driving in a single decoder. *arXiv preprint arXiv:2503.08612*, 2025.
- [69] Haochen Tian, Tianyu Li, Haochen Liu, Jiazhi Yang, Yihang Qiu, Guang Li, Junli Wang, Yinfeng Gao, Zhang Zhang, Liang Wang, et al. Simscale: Learning to drive via real-world simulation at scale. *arXiv preprint arXiv:2511.23369*, 2025.
- [70] Xiaoyu Tian, Junru Gu, Bailin Li, Yicheng Liu, Yang Wang, Zhiyong Zhao, Kun Zhan, Peng Jia, Xianpeng Lang, and Hang Zhao. DriveVLM: The convergence of autonomous driving and large vision-language models. *arXiv preprint arXiv:2402.12289*, 2024.
- [71] Jie Wang, Guang Li, Zhijian Huang, Chenxu Dang, Hangjun Ye, Yahong Han, and Long Chen. VGGDrive: Empowering vision-language models with cross-view geometric grounding for autonomous driving. *arXiv preprint arXiv:2602.20794*, 2026.
- [72] Junli Wang, Xueyi Liu, Yinan Zheng, Zebing Xing, Pengfei Li, Guang Li, Kun Ma, Guang Chen, Hangjun Ye, Zhongpu Xia, et al. MeanFuser: Fast one-step multi-modal trajectory generation and adaptive reconstruction via meanflow for end-to-end autonomous driving. *arXiv preprint arXiv:2602.20060*, 2026.
- [73] Xiaofeng Wang, Zheng Zhu, Guan Huang, Xinze Chen, Jiagang Zhu, and Jiwen Lu. DriveDreamer: Towards real-world-drive world models for autonomous driving. In *European conference on computer vision*, pages 55–72. Springer, 2024.
- [74] Xinyang Wang, Qian Liu, Wenjie Ding, Zhao Yang, Wei Li, Chang Liu, Bailin Li, Kun Zhan, Xianpeng Lang, and Wei Chen. Unifying language-action understanding and generation for autonomous driving. *arXiv preprint arXiv:2603.01441*, 2026.
- [75] Yuqi Wang, Xinghang Li, Wenxuan Wang, Junbo Zhang, Yingyan Li, Yuntao Chen, Xinlong Wang, and Zhaoxiang Zhang. Unified vision-language-action model. *arXiv preprint arXiv:2506.19850*, 2025.
- [76] Yin Wei, Zhang Chi, Chen Hao, Cai Zhipeng, Yu Gang, Wang Kaixuan, Chen Xiaozhi, and Shen Chunhua. Metric3D: Towards zero-shot metric 3D prediction from a single image. 2023.
- [77] Tianze Xia, Yongkang Li, Lijun Zhou, Jingfeng Yao, Kaixin Xiong, Haiyang Sun, Bing Wang, Kun Ma, Hangjun Ye, Wenyu Liu, et al. DriveLaW: Unifying planning and video generation in a latent driving world. *arXiv preprint arXiv:2512.23421*, 2025.
- [78] Zebin Xing, Xingyu Zhang, Yang Hu, Bo Jiang, Tong He, Qian Zhang, Xiaoxiao Long, and Wei Yin. GoalFlow: Goal-driven flow matching for multimodal trajectories generation in end-to-end autonomous driving. In *Proceedings of the Computer Vision and Pattern Recognition Conference*, pages 1602–1611, 2025.
- [79] Yifang Xu, Jiahao Cui, Feipeng Cai, Zhihao Zhu, Hanlin Shang, Shan Luan, Mingwang Xu, Neng Zhang, Yaoyi Li, Jia Cai, and Siyu Zhu. WAM-Flow: Parallel coarse-to-fine motion planning via discrete flow matching for autonomous driving. In *CVPR*, 2026.
- [80] Lihe Yang, Bingyi Kang, Zilong Huang, Xiaogang Xu, Jiashi Feng, and Hengshuang Zhao. Depth anything: Unleashing the power of large-scale unlabeled data. In *CVPR*, 2024.
- [81] Lihe Yang, Bingyi Kang, Zilong Huang, Zhen Zhao, Xiaogang Xu, Jiashi Feng, and Hengshuang Zhao. Depth anything V2. *arXiv:2406.09414*, 2024.
- [82] Zhenjie Yang, Yilin Chai, Xiaosong Jia, Qifeng Li, Yuqian Shao, Xuekai Zhu, Haisheng Su, and Junchi Yan. DriveMoE: Mixture-of-experts for vision-language-action model in end-to-end autonomous driving. *arXiv preprint arXiv:2505.16278*, 2025.
- [83] Zhenjie Yang, Xiaosong Jia, Qifeng Li, Xue Yang, Maoqing Yao, and Junchi Yan. Raw2Drive: Reinforcement learning with aligned world models for end-to-end autonomous driving (in CARLA v2). In *The Thirty-ninth Annual Conference on Neural Information Processing Systems*, 2025.
- [84] Yuqi Ye, Zijian Zhang, Junhong Lin, Shangkun Sun, Changhao Peng, and Wei Gao. AutoDrive-P3: Unified chain of perception-prediction-planning thought via reinforcement fine-tuning. *arXiv preprint arXiv:2603.28116*, 2026.

- [85] Rui Yu, Xianghang Zhang, Runkai Zhao, Huaicheng Yan, and Meng Wang. DistillDrive: End-to-end multi-mode autonomous driving distillation by isomorphic hetero-source planning model. In *Proceedings of the IEEE/CVF International Conference on Computer Vision*, pages 26188–26197, 2025.
- [86] Zhenlong Yuan, Chengxuan Qian, Jing Tang, Rui Chen, Zijian Song, Lei Sun, Xiangxiang Chu, Yujun Cai, Dapeng Zhang, and Shuo Li. AutoDrive-R2: Incentivizing reasoning and self-reflection capacity for VLA model in autonomous driving. *arXiv preprint arXiv:2509.01944*, 2025.
- [87] Shuang Zeng, Xinyuan Chang, Mengwei Xie, Xinran Liu, Yifan Bai, Zheng Pan, Mu Xu, and Xing Wei. FutureSightDrive: Thinking visually with spatio-temporal CoT for autonomous driving. *arXiv preprint arXiv:2505.17685*, 2025.
- [88] Xiaohua Zhai, Alexander Kolesnikov, Neil Houlsby, and Lucas Beyer. Scaling vision transformers. In *Proceedings of the IEEE/CVF conference on computer vision and pattern recognition*, pages 12104–12113, 2022.
- [89] Bozhou Zhang, Nan Song, Xin Jin, and Li Zhang. Bridging past and future: End-to-end autonomous driving with historical prediction and planning. In *Proceedings of the Computer Vision and Pattern Recognition Conference*, pages 6854–6863, 2025.
- [90] Bozhou Zhang, Nan Song, Jingyu Li, Xiatian Zhu, Jiankang Deng, and Li Zhang. Future-aware end-to-end driving: Bidirectional modeling of trajectory planning and scene evolution. In *NeurIPS*, 2025.
- [91] Jinqing Zhang, Zehua Fu, zelinxu, wenying.dai, Qingjie Liu, and Yunhong Wang. ResWorld: Temporal residual world model for end-to-end autonomous driving. In *The Fourteenth International Conference on Learning Representations*, 2026.
- [92] Kaiwen Zhang, Zhenyu Tang, Xiaotao Hu, Xingang Pan, Xiaoyang Guo, Yuan Liu, Jingwei Huang, Li Yuan, Qian Zhang, Xiao-Xiao Long, Xun Cao, and Wei Yin. Epona: Autoregressive diffusion world model for autonomous driving. In *Proceedings of the IEEE/CVF International Conference on Computer Vision (ICCV)*, 2025.
- [93] Lingjun Zhang, Yujian Yuan, Changjie Wu, Xinyuan Chang, Xin Cai, Shuang Zeng, Linzhe Shi, Sijin Wang, Hang Zhang, and Mu Xu. MindDriver: Introducing progressive multimodal reasoning for autonomous driving. *arXiv preprint arXiv:2602.21952*, 2026.
- [94] Rui Zhao, Yuze Fan, Zigu Chen, Fei Gao, and Zhenhai Gao. DiffE2E: Rethinking end-to-end driving with a hybrid diffusion-regression-classification policy. In *The Thirty-ninth Annual Conference on Neural Information Processing Systems*, 2025.
- [95] Zhida Zhao, Talas Fu, Yifan Wang, Lijun Wang, and Huchuan Lu. From Forecasting to Planning: Policy world model for collaborative state-action prediction. In *Advances in Neural Information Processing Systems*, 2025.
- [96] Yupeng Zheng, Pengxuan Yang, Zebin Xing, Qichao Zhang, Yuhang Zheng, Yinfeng Gao, Pengfei Li, Teng Zhang, Zhongpu Xia, Peng Jia, XianPeng Lang, and Dongbin Zhao. World4Drive: End-to-end autonomous driving via intention-aware physical latent world model. In *Proceedings of the IEEE/CVF International Conference on Computer Vision (ICCV)*, pages 28632–28642, October 2025.
- [97] Zhiyu Zheng, Shaoyu Chen, Haoran Yin, Xinbang Zhang, Jialv Zou, Xinggang Wang, Qian Zhang, and Lefei Zhang. ResAD: Normalized residual trajectory modeling for end-to-end autonomous driving. *arXiv preprint arXiv:2510.08562*, 2025.
- [98] Zewei Zhou, Tianhui Cai, Yun Zhao, Seth Z. and Zhang, Zhiyu Huang, Bolei Zhou, and Jiaqi Ma. Au-toVLA: A vision-language-action model for end-to-end autonomous driving with adaptive reasoning and reinforcement fine-tuning. *arXiv preprint arXiv:2506.13757*, 2025.
- [99] Jialv Zou, Shaoyu Chen, Bencheng Liao, Zhiyu Zheng, Yuehao Song, Lefei Zhang, Qian Zhang, Wenyu Liu, and Xinggang Wang. DiffusionDriveV2: Reinforcement learning-constrained truncated diffusion modeling in end-to-end autonomous driving. *arXiv preprint arXiv:2512.07745*, 2025.